A retarding field energy analyser for the JET plasma boundary

R. A. Pitts and R. Chavan

Centre de Recherches en Physique des Plasmas, Association EURATOM-Confédération Suisse, Ecole Polytechnique Fédérale de Lausanne, CH-1015 Lausanne, Switzerland

S. K. Erents, G. Kaveney, G. F. Matthews, G. Neill, J. E. Vince, and the JET-EFDA workprogramme contributors[a)]

Euratom/UKAEA Fusion Association, Culham Science Centre, Abingdon, OX14 3DB, UK

[a)]See annex of J. Pamela et al., "Overview of recent JET results and Future Perspectives", Fusion Energy 2000 (Proc. 18th Int. Conf. Sorrento, 2000), IAEA Vienna (2001)

I. Duran

Institute of Plasma Physics, Association EURATOM/IPP.CR, Praha 182 21, Czech Republic

Retarding field analysers (RFA) are essentially the only practical tool with which to measure the distribution of ion energies in the boundary plasma of magnetic fusion devices. The technique has long been attempted in such facilities with varying degrees of success, but, by virtue of the delicate nature of these material probes and the hostile environment in which they are inserted, its use has been limited to smaller plasma machines with easier access and more tolerable plasma conditions. This contribution describes in detail a new RFA probe head recently constructed and tested on the large JET tokamak facility and now being used for plasma physics studies. Emphasis is placed on the details of design and mechanical construction as they relate to the particularly harsh conditions imposed both by the JET boundary plasma and the requirement that the probe be used to sample this plasma by insertion via a multiple plunge, fast reciprocating drive system. Some preliminary physics results are also included demonstrating both successful operation of the new device and discussing its limitations.

I. INTRODUCTION

Ion temperatures, T_i, and velocity distributions, f(v), in the plasma edge of fusion devices are notoriously difficult to measure and thus rarely available but yet are important plasma boundary quantities. Spectroscopic observations of hydrogenic isotopes usually comprising the main plasma species are useful and somewhat easier to perform, but cannot yield the fuel ion T_i directly since the the hydrogenic fuel ions do not emit photons. Instead, assumptions, or modelling are required to determine the degree of ion-neutral coupling. In contrast, the Retarding Field Analyser (RFA) offers an alternative approach that can access the plasma ion or electron velocity distribution directly and has been successfully demonstrated in a number of plasma machines, with[1-6] and without[7-8] confining magnetic fields. In the former case and the one that will be concerned by this contribution, the probe is generally designed to measure the component of charged particle velocity parallel to the field direction, $f(v_{||})$. The use of these probes presents special difficulties, not the least of which being the obvious materials and power handling problems posed by the immersion of a material object into a plasma, particularly where high power flux densities may be present. On the large JET tokamak, for which the probe described here has been designed and implemented, issues of reliability (the diagnostic cannot easily be accessed once installed) and an ambient operating temperature of ~200°C must also be addressed. Indeed, the high power fluxes characteristic of the JET plasma boundary necessitate a fast reciprocation movement to periodically insert the probe for brief intervals. This in turn imposes further restrictions on the probe design.

II. RFA PRINCIPLE

Figure 1 illustrates the basic principle of RFA operation. Charged particles are transmitted through an aperture and are analysed by retardation in the electric field established through bias potentials applied to a number of grids. In the tokamak edge plasma, the probe head containing the RFA electrodes is aligned along the total magnetic field such that the parallel component, $f(v_{||})$, of the charged particle velocity distribution is the sampled quantity. The entrance slit must be wide enough to permit adequate flux transmission, yet sufficiently small that the electrostatic sheath established around the slit edges be large enough to bridge the aperture width and hence shield the aperture from the plasma[3,9]. This implies slit widths of the order of the Debye length which, in the tokamak edge plasma, is typically of order several 10's of microns.

Once inside the device, particles are subject to a swept retarding potential on Grid 1 which

ranges from zero to large positive (negative) values if ions (electrons) are the sampled quantity. Grid 2 is then appropriately biased to reject the species not required, with the collector usually held at a potential such that secondary electrons released by primary ion or electron impact there are returned to its surface and make no contribution to the total collected current. Since the electron velocity distribution (and hence the electron temperature, T_e) can to some extent be measured by the simple single Langmuir probe, the primary focus of RFA application is often the ion velocity distribution. An appropriate electrode bias configuration for ion analysis is included in Fig. 1, illustrating how the slit plate is normally negatively biased to repell all but the highest energy electrons. A positive voltage sweep is applied to Grid 1 and a constant negative bias on Grid 2 at a value lower than that applied to the slit eliminates any remaining electrons. The collector at zero volts suppresses any ion induced secondary electrons.

More refined approaches to ion-mode RFA analysis would likely reject primary electrons with Grid 1, sweep Grid 2 and provide a third grid with constant negative bias to repel any secondary electrons produced by ion impact on Grids 1,2. However, for the relatively low ion energies characteristic of most tokamak edge plasmas and high transparency grids, such ion induced secondary electron emission is neglibible in comparison to that occurring at the collector surface itself. Given the tight space restrictions (see below) imposed on fusion plasma probes, the opportunity to exclude a further electrode is a welcome advantage.

In the electron RFA mode, the negative voltage sweep is applied to Grid 1, with Grid 2 held at a large positive potential, the collector at zero volts and the slit allowed to float. Here, a third grid is more important, since secondary electrons induced by primary electron impact on the collector cannot be effectively suppressed without biasing the collector iself to large positive potentials. Although the JET RFA has been successfully tested in electron mode, results are not discussed here.

In most fusion applications, the bias potentials are applied with respect to a common ground defined by the potential of the tokamak vacuum vessel. This can be inconvenient, however, in the case of reciprocating probe systems such as that described here in which the local floating potential adopted by the probe head can change appreciably as the probe moves deeper into the plasma.

Returning to the ion analysis mode of operation, the current-voltage characteristic formed by the positive voltage sweep, V_1, and the ion collector current, I_c, is a measurement of the integral ion parallel velocity distribution:

$$I_c = Aq_i \int_u^\infty v_{||} f(v_{||}) dv_{||} \quad (1)$$

with A a normalisation constant, $q_i = eZ_i$ the ion charge and $u = \sqrt{2q_i V_1 / m_i}$ where m_i is the ion mass. Though $v_{||}$ can in principle be unfolded from numerical differentiation of the characteristic given by Eq. (1), tokamak signals are often too noisy for this method to be of any practical use. Fortunately, the velocity distribution is often experimentally found to be closely approximated by a Maxwellian shifted in velocity space by an amount equal to that gained by acceleration in the sheath and pre-sheath electric fields[2-5] (see also section V). In this case, for values of V_1 exceeding the voltage required to back off this energy shift, the I-V characteristic can be written in the form:

$$I_c = I_i \exp\left(-\frac{Z_i V_1}{T_i}\right) \quad (2)$$

where $I_i = AZ_iT_ie^2/m_i$ and T_i (in eV) is the ion temperature of the distribution. In practice, an iterative numerical procedure combined with an appropriate fitting algorithm may be used to identify both T_i and the voltage shift corresponding to the sheath potential fall in a single fit to any given I-V characteristic[1,9-10].

III. PROBE DESIGN

The rather high power fluxes flowing parallel to the magnetic field (as high as several 10's MWm^{-2} but typically ~ 10 MWm^{-2}) require fast insertion of the probe head into the plasma for short durations. This is accomplished on JET by any one of two reciprocating probe drive systems[11] on top of the torus located as shown in Fig. 2. A fast pneumatic system can drive the probe head into the plasma covering a return distance of ~40 cm in ~300 ms at 2 s intervals. Together, physics, heat flux and mechanical constraints place a number of requirements on the RFA head design:

- To account for the influence on T_i of the strong plasma flows known to be present in the JET scrape-off layer (SOL)[12], bi-directionality is required - the probe head must contain an RFA sampling plasma in both directions along the total magnetic field. A similar device, named the Janus probe, was employed for the first time on the circular Alcator tokamak[5], but was not deployed on a reciprocating drive, remaining instead in the limiter shadow on a

retractable slow drive system.

- Alignment of the probe to within a few degrees of the local magnetic field must be guaranteed. This requires orienting the probe head correctly in each of the (φ,R) and (φ,z) planes, where (R,φ,z) define a toroidal coordinate system with φ the toroidal angle, z the vertical axis through the centre of torus and R the radius vector (Fig. 2 is the (R,z) plane or "poloidal" cross-section).
- The probe head external diameter must not exceed 40 mm for compatibility with the JET reciprocating drives. At this diameter, the probe would necessarily be classed as a "large probe" on smaller tokamaks in the sense that the disturbance caused by the probe insertion into a fully ionised, strongly magnetised plasma can significantly modify the very parameters it is designed to measure. To first order, the degree of disturbance may be quantified analytically[13] in terms of the natural, ambipolar collection length, L_{col}, for an electrically floating object of square dimension, x: $L_{col} = x^2 c_s / 8D_\perp$ with c_s the isothermal ion sound speed in the plasma edge ($c_s = \sqrt{e(T_e + Z_i T_i)/m_i}$, T_i, T_e in eV) and $D_\perp$ the anomalous, ambipolar cross-field diffusion coefficient. Assuming x = 0.04 m, $T_i = T_e = 50$ eV and $D_\perp = 1$ $m^2 s^{-1}$, $L_{col} \sim 14$ m for the RFA. In JET, for most of the SOL width of interest, this is considerably shorter than the magnetic connection length along field lines from the probe location to the next solid surface (the divertor targets). This distance is ~70 m to the inner, high field side target and ~40 m to the outer target for typical JET combinations of plasma current, I_p and toroidal magnetic field, B_φ (2.0 MA and 2.0 T respectively). In this case, the probe, although it can only strictly measure a spatial average of any quantity along the length of flux tube determined by L_{col}, is unlikely to be sufficiently disturbing that the magnetic SOL it creates when inserted is not reasonably close to that prevailing in its absence.
- An extremely narrow entrance slit must be provided to ensure both that high currents in the device do not lead to space charge accumulation and that ions are extracted from the plasma unaffected by collective effects that would occur if the slit were not rendered invisible to the plasma by the electrostatic sheath. The slit must be incorporated into a bulk support providing adequate power handling under plasma exposure.
- Adequate pump-out must be provided for neutral gas which may build up in the RFA cavity as the probe heats up during insertion.
- The delicate RFA electrodes must of course be surrounded by a protective housing, itself

capable of surviving the plasma heat flux during normal exposure and “off-normal” events and the mechanical forces induced by the fast reciprocation.

- For application on JET, the entire probe head must be modular, allowing the same reciprocating drives to be used for the exposure of many different probe types.

Figure 3 presents, in exploded, isometric form, the RFA probe head design that satisfies the above criteria and which has been successfully deployed in the JET plasma boundary (see Sect. V). It represents the result of several improvements to a basic design concept that has been refined over a period of several years - the size and complexity of the JET facility renders prototyping steps extremely arduous and time consuming. Preliminary physics results and some brief details of an earlier version of this device have been reported by Guo[14]. In the technical description that follows, the reader is invited to refer to the numbers assigned to the important components in Fig. 3.

A. PROBE BODY

The ~30 cm long main probe body (1) is machined from a single bar of hot-pressed boron nitride (BN AX05, Sintec Keramik (UK) Ltd., Newport, UK) which has been certified as free of mechanical defects by appropriate X-ray testing. This material is now used for all JET reciprocating probe heads as a replacement for the previous CFC designs. Boron nitride has both a large volume resistivity and an essentially zero coefficient of thermal expansion. The former is of particular importance in limiting the flow of current through a conducting (such as CFC) probe body in the event of off-normal events, such as rapid vertical instabilites of the tokamak plasma which can lead to the generation of “halo” currents. Such currents, flowing across the strong confining magnetic field in JET (typical values of the main confining field at the probe location are ~2T) can lead to large jxB forces and subsequent probe fracture. The low thermal expansion coefficient is put to good advantage by arranging for the Inconel 625 support (2) that interfaces the probe body to the drive system to be placed internally rather than externally. Two retaining screws (3) connect the body and support (via location sleeves and an internal location ring containing threaded holes in a spark eroded flat internal bore), but exert no clamping force throughout the operating temperature range. During operation (the JET vacuum vessel is continuously baked at temperatures in the range 200 - 320°C), the Inconel expands but the BN does not. Tolerances on the machining of the Inconel support and BN body are arranged so that

the fit is closer at 300°C than at room temperature but not so close that bursting forces are induced in the BN.

Low thermal expansion also implies a desirable resistance to thermal stress fracture, but BN does not have the flexural strength of CFC. An exhaustive series of tests have been performed on real probe body geometries to determine the suitability for use at JET. The reciprocation cycle in plasma has been simulated by exposing samples in the JET Neutral Beam test facility[15] to hundreds of heat pulses in the range 5-40 MWm^{-2} with durations of ~3 s to 200 ms respectively. Certified shock testing along three perpendicular axes at ambient temperature and at 180°C has also been executed up to 30g for 6 ms without sample destruction. Typical maximum accelerations during real reciprocations are only of order 1-2g.

B. RFA CAVITIES: GRIDS AND ENTRANCE APERTURE

The bi-directional RFA itself is formed by a compact electrode stacking arrangement using a backing support (4) machined out of the BN probe body itself. The electrodes are guided using 1.6 mm diameter threaded stainless steel support spindles, electrically isolated with machineable glass ceramic tubes (MACOR®, Fiberoptic, Spreitenbach, Switzerland) and secured by locknuts against the slit plate structure. Beginning with the high purity molybdenum (10x15 mm) collector plates (5), the stack comprises three grids (6) and a slit plate (7), with the grids separated by delicate, forked insulating spacers machined in pyrolytic boron nitride (8). The latter has a layered structure which is easy to machine and is strong under compressive stress. Molybdenum was chosen as collector plate material in the hope that a technique of in-situ measurement of ion and electron secondary electron emission using the RFA and first pioneered on the DITE tokamak[16], might be re-attempted at JET. Such measurements have not yet, however, been possible at the time of writing.

Grid separation is largely determined by space restrictions and technical feasibility and is fixed at s = 2 mm, giving equispaced electrodes in each RFA cavity. Along with the parallel ion energy and applied voltage, the distance, s, between the conducting planes represented by the grids is an important parameter determining the extent to which axial space-charge inside the device may eventually create a potential hill large enough to reflect the primary ions, independently of the specifically applied grid and collector voltages. Estimating the maximum permissible current density within the RFA cavity before such effects become important is extremely difficult, though some analytic expressions have been offered[6,10], based on the

classic early work of Langmuir[17]. Nachtrieb[18], has also considered in detail the problem from the point of view determining a current limit set by the electrostatic self-potential of the ion beam when the former is of the order of the average beam energy itself. A full treatment requires a solution of Poisson's equation in three dimensions, self-consistently accounting for the distribution of charge density due to individual particle orbits. This has not yet been attempted for the JET device, though as Sect. V will show, there is evidence that under certain plasma conditions, space-charge effects may be having a strong impact on the collector currents. Issues of beam divergence due to the build-up of radial fields generated by space-charge are not important for retarding field analysers since these radial fields do not affect the quantity of interest - the axial ion energy - although they are important when estimates of the ion charge density are required (Sect. V).

In addition to the two principle retarding grids, a third is pressed up against the rear of the slit plate by the stacking arrangement and is in good electrical contact with the slit. Its purpose is to render the electric field behind the slit plate itself as planar as possible, providing uniform potential surfaces within the RFA cavity. This is particularly important in view of the non-planar nature of the slit plate at its rear surface (see below). All grids are manufactured in beryllium-copper (BeCu) and are produced by photolithography in a foil of thickness 25 μm with etching from both sides (Photofabrication Services Ltd., St. Neots, UK). This material has been chosen primarily for its relative stiffness, even in thin foils, providing for greater resistance to bending at elevated temperatures and under the reciprocation forces. It also has the added benefit of being non-magnetic.

The grid region itself is etched as a rectangular area 6x3 mm bounded by two half-circular regions with radius 3 mm providing for a total area ~46 mm^2. The orientation of the grid mesh itself is carefully arranged to be diagonal to the vertical entrance slit so that no single grid wire can completely block the path of particles entering the device. Grid wires of 40 μm width are distributed on a matrix of square grid cells with wire separation of D = 0.4 mm giving a mark-space ratio of 10 and a geometric transmission of $T = (D - 2r_0)^2/D^2 \sim 0.81$, ($r_0 = 20$ μm). For an ion attracting grid (such as Grid 2 in Fig. 1 when the RFA is in ion analysis mode), this transmission factor is likely to be modified due to perturbation of those ion trajectories passing close to grid wires. An effective grid wire radius, $r_{eff} = r_0(1 + V/V_0)^{1/2}$, with V the grid potential and V_0 the initial ion energy can be derived from cylindrical probe theory for this case[10]. For the -200 V electron retarding potential normally applied to Grid 2 and an ion of

energy 50 eV, the ideal transmission factor is reduced to 0.60. Trajectory defocussing can also be an issue in some cases and can limit the energy resolution of a retarding grid due to transfer of perpendicular and parallel momentum. The extent to which this occurs can be expressed approximately in terms of the relative change in ion energy, E in passing through the grid aperture as[19]: $\frac{\Delta E}{E} \approx \frac{D^2}{16s^2}$ ~ 0.25% for the JET RFA grids and therefore insignificant.

These are clearly only qualitative considerations and do not include such effects as particle acceleration and decceleration near grids which leads to transfer of perpendicular and parallel energy and hence modification of Larmor orbits and beam sizes. More quantitative estimates would require a Monte Carlo numerical treatment of the sort performed by Wan[20], accounting for the full distribution of particle velocities and grid potentials, including ion acceleration through the sheath potential. Such analysis has not been performed for the JET probe but Wan finds only weak perturbations in the parallel energy distribution function for grid geometries and biasing schemes very similar to those employed at JET.

Each grid comprises a lower tab providing two 3 mm diameter holes through which the support spindles pass. In the case of Grids 1,2, this tab is extended to one side and folded through 90° over the end of a small block forming one half of a dedicated cable clamp (9) which ensures electrical connection between the grid and the wire bringing the applied voltage. An appropriate radius on the block edges ensures that grid tab is not excessively stressed during the mechanical forces imposed by probe reciprocation.

The final component in the electrode stack is the slit plate. For a device operating in the tokamak edge, the aperture plate is the most critical element - it must perform the dual function of non-perturbing particle selection into the RFA cavity and as first barrier to the extremely high heat fluxes that would otherwise destroy the delicate internal components. As Section II has described, the slit itself must be wide enough to ensure transmission of adequate current into the probe but yet small enough that the electrostatic sheaths formed at the slit edges be able to bridge the gap offered by the slit width, effectively rendering the aperture invisible to the plasma. In this case, particles passing through the slit will be representative of those arriving anywhere on the probe surface.

Ideally, then, the entrance slit width, w, should satisfy the condition $w \ll 2\lambda_D$ where $\lambda_D = \left(\frac{\varepsilon_0 T_e}{e n_e}\right)^{1/2}$ is the Debye length (T_e in eV) and is a lower limit for the approximate sheath thickness. For typical conditions (ohmic and L-mode) near the separatrix in the JET plasma boundary (T_e ~ 30 eV, n_e ~ $5x10^{18}m^{-3}$), λ_D ~ 20 μm. More detailed kinetic analysis assuming

a source-free sheath and including the effects of secondary electron emission[21] shows in fact that the sheath has a slightly greater extent (for floating wall conditions), than a single Debye length, especially if a negative bias is applied to the surface (as is common when performing RFA ion analysis). In practice, the condition on slit width may be relaxed somewhat, such that $w = 1 \rightarrow 2\lambda_D$ is more likely to be appropriate[9].

Providing for a well defined slit only a few microns wide in a high heat flux component is a considerable challenge. Photo-lithographic procedures (as employed for the BeCu grids described above) can easily produce such slits with excellent definition in thin foils which can then be bonded to a suitable substrate[9], but this technique fails even under moderate heat fluxes due either to foil melting or loss of adhesion to the substrate. For the JET device, the approach has been to seek a mono-block solution in which the slit is an integral part of the slit plate itself. The plate is first machined to the correct dimensions and then a pocket is spark-eroded into the rear with 12° and 30° tapered surfaces terminating along a narrow slot 3 mm in length and 30 μm from the back surface of the plate. The slot is then opened completely using laser cutting to precisely define the slit edges and define an effective knife edge with nominal dimension 3x0.03 mm. Such a knife edge has a structure which facilitates the conduction of heat out into the slit plate body thus reducing the absolute temperature rise in the slit vicinity. The chamfered opening behind the slit also enlarges the overall aperture for transmission once the gyrating particles pass through the slit itself.

The two-stage process of spark erosion (Wines, Sevenoaks, UK) followed by laser cutting (AEA Technology, UK) was successfully performed to manufacture Inconel 600 slit plates in a prototype RFA probe head which was the direct precursor to the device described here. Unfortunately, Inconel turns out to be insufficiently robust for use in the JET plasma boundary. The material used has a melting point of $T_m = 1663$ K, but in practice, such temperatures should never be approached during use if unavoidable phase changes in the alloy, particularly in the vicinity of the tiny entrance slit, are to be avoided.

Following first use on JET, finite element simulations, an example of which is shown in Fig. 4, demonstrated that for even relatively modest heat flux profiles (previously measured using a separate reciprocating Langmuir probe at the same poloidal location in the JET SOL), the temperature rise in the slit region would be intolerably high. An alternative material was therefore sought and found in the form of the high refractory alloy, TZM (Plansee, Reutte, Austria) comprising the elements Mo:Ti:Zr for which the average nominal chemical

composition in weight is 99:0.5:0.1% (atomic numbers 42:22:40). Finely dispersed Ti-carbides give this material excellent strength properties up to 1773 K, with the material itself having T_m = 2773 K. The alloy has a thermal diffusivity about 10 times higher than Inconel 600, such that for the expected highest heat fluxes near the separatrix, the maximum temperature rise of a TZM slit is some 900 K compared with ~1300 K for Inconel 600 (Fig. 4). This is well within the operational limits of the material. The use of TZM also offers greater protection against unanticipated "off-normal" events, during which higher than predicted heat fluxes might otherwise lead to slit plate melting in the case of Inconel. Although the probe cannot make meaningful measurements during such events, it must be able to withstand the increased heat flux if it occurs during a fast reicprocation.

The mono-block slit plates have a geometrical form carefully designed to provide a rounded contour and to provide sufficient mass for heat conduction away from the slit area which is directly exposed to the plasma power flux. Unlike the grids and grid separators, the aperture plates are not geometrically identical - they are individually shaped to account both for the bi-directional nature of the RFA and the specific orientation of the total magnetic field direction in the tokamak.

C. PROBE HEAD ALIGNMENT

The probe head must be aligned as perpendicularly as possible to the field direction so that it is the parallel ion or electron velocity which is measured and not some component of it. Because the tokamak magnetic field is comprised of a poloidal and toroidal component, the field lines follow a helical trajectory around the machine and a probe sampling the edge plasma from a given location must ideally be aligned in each of the (φ,R) and (φ,z) planes. Alignment in the (R, z) plane (ie to the poloidal plasma contour) is not important for a device like the RFA with recessed slit plates in a protective housing.

Figure 5 illustrates more clearly than the isometric projection in Fig. 3 how probe alignment in the (φ,z) plane is achieved by pre-machining the BN RFA stack support (item (4) in Fig. 3) to an angle of 6° to the central axis of the probe head. This angle, computed as $\tan^{-1}(B_z/B_\varphi)$ is typical of the field line trajectories for most of the discharges into which the probe is inserted. It varies little over the ~20 cm stroke of the probe during reciprcocation. For the large majority of experimental campaigns, JET operates with I_p and B_φ in the clockwise direction looking from the top of the machine. This gives a total magnetic field line trajectory rotating in the direction

of a corkscrew moving forward toroidally so that field lines twist round from outer to inner divertor and move up towards the probe. For clockwise I_p, the conventional, though now less frequently used terminology, puts the RFA entrance aperture looking clockwise on the "ion" or i-side, namely the side facing the drift direction for positive charges accelerated by the tokamak toroidal electric field. This side also therefore faces plasma flowing along field lines to or from the outer divertor in the SOL. Similarly, the opposite side of the RFA faces the inner divertor target and is the "electron" or e-side of the probe.

The various combinations of I_p and B_φ also yield an angle in the (φ,R) plane, $\tan^{-1}(B_R/B_\varphi)$ ~ 8° which is fixed by keyway slots ((10) in Fig. 3) machined into the Inconel probe body support (2) and the aluminium-bronze sleeve (11) that provides the interface to the reciprocating drive shaft. In fact, even when JET operates with reversed toroidal field, the magnetic field line topology is preserved by also reversing the plasma current direction in order to avoid overheating of divertor target protection tile leading edges which are specifically optimised for power handling in a given magnetic helicity. The RFA may thus be used for measurements in both reversed and forward B_φ.

D. RFA CAVITY HOUSING AND CABLE CONNECTION

The entire RFA electrode stack is enclosed in a protective BN AX05 housing (item (9) in Fig. 3) in which two machined apertures are provided for plasma access to the slit plates and which fixes the slit centre at a distance of 9 mm from the leading edge of the housing. This cylindrical probe cap has a nominal maximum wall thickness of 1 cm, but the internal geometry of the housing has a complex three-dimensional form to provide, as far as possible, for a close fit around the entirety of the electrode stack. This was motivated by early experiments with a more crude device in which rather strong apparent breakdown in the probe collector currents was indicative of considerable outgassing as the probe heated up during insertion into the plasma. The rounded slit plate edges alluded to earlier, form a contour also followed by the electrode stack so that cap slides easily onto a curved structure.

Two series of three 2 mm diameter pumping holes are drilled into the extremity of the housing directly above the closed internal cavity represented by each side of the RFA to assist in outgassing. The diameter is estimated using the simple gas conductance equation for molecular flow and requiring that the pressure, p in the RFA cavity of volume V, fall back to its pre-reciprocation value, p_0, in a given time, t, where

$$t = \frac{V\alpha \ln\alpha}{C(\alpha - 1)} \tag{3}$$

with $\alpha = p/p_0$ and C the conductance of the cylindrical hole, diameter, d and length, l for mass species, m: $C = \left(\frac{\pi RT}{2m}\right)^{1/2} \frac{d^3}{(4d + 3l)}$. For $p/p_0 = 30$, V = 0.6 cm^3, d = 0.2 cm, l = 0.3 cm and T = 200°C (the approximate probe ambient operating temperature), Eqn. (3) gives t ~ 4 ms.

Two screws with rectangular nuts and specially manufactured Inconel X750 washers locate the housing on the probe body using the same principle of relative thermal expansion as for the probe body and drive shaft support to avoid clamping forces. The entire housing is painted with a colloidal graphite layer ~100 μm thick which is later impregnated into the BN surface by baking in atmosphere at ~150°C followed by wiping with alcohol to remove excess carbon which otherwise leads to too high an outgassing rate under vacuum. This process avoids coating the exposed surface of the slit plates with insulating boron nitride via sputtering action of the impinging plasma ions on the neighbouring cap surface. The exposed area itself comprises a rectangular opening of dimension 4x6 mm with chamfered edges opening out into the cap and filed out by hand following cap machining and before graphite painting. In principle, such chamfering is performed in order to prevent preferential removal of ion orbits by the side walls of the cap opening which may lead both to velocity selection and the establishment of strong local electric fields potentially modifying particle trajectories. Just such “tunnel” effects have recently been observed and modelled with kinetic simulations[22]. In the case of the JET RFA, the maximum possible opening compatible with power handling in the high heat flux region of the slit plates has been provided.

From their clamping points at the foot of the RFA electrodes, in-house manufactured signal cables are transmitted down the cylindrical hollow machined inside the probe body. They are coaxial in form, comprising a central GLIDCOP® (OMG Americas) conductor (a copper-boron alloy characterised by low creep at elevated temperatures) surrounded by a fibre glass insulating sheath and then a braided stainless-steel outer shield. In each case, the coaxial body is terminated and sealed at each end, leaving an appropriate length of central conductor for electrical connection. The termination is performed by small, tight fitting steel caps, together with Ceramabond 751 ® (Aremco Products, Inc., US) sealant which is applied prior to a light air bake to ~100°C.

The cables are guided through the probe body by three BN AX05 spacers (item (12) in Fig. 3) which serve to provide both rigidity and to separate the two cables connected to the collector

plates via slots milled along the length of each insulator. This separation permits the application of bias potentials to the collectors for use in RFA mode for suppression of secondary electrons (see Section II) or, in more advanced modes, for the measurement of the secondary emission itself. With the exception of the collectors, all cable screens are connected together at a single point which may then be carried away from the probe head via a dedicated earthing cable. This forms the ninth signal output (2 slits, 4 grids and 2 collectors) and employs all nine cables provided for in the current JET probe drive systems.

At the rear of the probe body, a pair of MACOR insulating disks (13) serves to secure the coaxial cable ends and then to provide a means for spreading of the individual conductors allowing for easier connection to the final pin arrangement which is standard for the JET reciprocating probe drives and permits relatively straightforward permutation of a variety of probe heads. The Alumel terminating pins and pyrolytic BN C-washers (a combination used for its tendency not to seize at high temperatures) are housed within a final MACOR disk (14) which is also fitted with two OHFC copper screen plugs ensuring separate electrical connection to the collector cable outer screens. All three disks are housed with the Inconel probe body support (2), itself carrying three aluminium-bronze location plungers with Inconel X750 spring washers (15) forming spring latches onto the aluminium-bronze sleeve (11) which is mounted on the end of main probe drive shaft and provides a low friction interface to the probe head support. The photographs in Fig. 6 illustrate both the internal RFA cavities and the complete probe head comprising the BN probe body and protective housing together with the main reciprocating drive shaft interface.

IV. ELECTRONICS

Although there are a few features specific to the RFA probe head, much of the electronics infrastructure is generic to the JET fast reciprocating probe systems and must be shared by all probe heads using them. Fig. 7 gives a schematic illustration of the configuration used for the RFA.

To minimise noise and the effects of cable capacitance, each JET probe drive is equipped with nine fully triaxial cables extending from the head flange down to the probe head interface, though, in the case of the RFA, only the two collector signals fully utilise the triaxial facility. The other cables have both outer shields grounded at the tokamak vacuum vessel potential, which is the reference ground for the signal conditioning cubicle located ~100 m away from the

probe itself. All plant signals are passed through unity gain isolation amplifiers, guaranteeing both safety and isolation of the cubicle from the separate building earth of the JET CODAS data acquisition system.

Slit, collector and grid bias are largely provided by Kepco BOP-100M operational amplifiers (Kepco, Inc, USA) with appropriate series protection resistors if necessary. The high voltage ramp for grid sweeping is generated by a custom-built, low current amplifier with input driving waveform supplied by an EPROM clocked at the data acquisition rate. Bandwidth limitations imposed by the long cable lengths from torus to cubicle require a head amplifier near the probe location for measurement of RFA collector currents at the microampere level. This unit consists of a floating current amplifier input stage (to allow the application of bias potentials to the collectors if required), followed by an isolation stage and a simple output unity driver. Its bandwidth is relatively limited at ~5 kHz but the acquisition rate is itself in any case currently restricted to 10 kHz.

V. EXAMPLE RESULTS

It is appropriate to present selected results from the RFA described above, though detailed physics analysis is beyond the scope of this contribution and will be addressed elsewhere. In fact, one of the principle difficulties in designing and using edge probes of this sort in a large facility such as the JET tokamak is the relatively limited experimental time available and the inaccessibility of the diagnostic once installed. Mechanical or electrical faults inside the probe head have long lead times before any kind of repair, or even simple observation can be effected, notably due to low levels of radioactive contamination (mostly tritium due to its previous use in JET) and trace amounts of beryllium that are deposited on the probe during reciprocations into plasma (beryllium evaporation onto internal vacuum vessel wall surfaces is regularly performed at JET as a method of gettering to reduce oxygen levels in the tokamak plasma). As a consequence, measurement time must be optimised and there is little scope for the many interesting (and important) tests that can be made on analyser function with respect to performance, grid and slit transmission, space charge effects etc.

The compilation in Fig. 8 demonstrates the typical results obtained with the device in a single JET diverted discharge (I_p = 2.0 MA, B_φ ramped from 2.0 $\rightarrow$ 1.5 T) into which the RFA was inserted at three times separated by 2 s intervals during the ohmic heating phase of the pulse; neutral beam injection (NBI) is added later, as evidenced by the increase of density after t = 24

s. Although the total vertical plunge of the probe head is some 20 cm in this case (from ~1.75 → 1.55 m above the vacuum vessel midplane), useable current is only detected over ~8 cm at the probe location corresponding to a sampling period of ~200 ms. The third reciprocation penetrates slightly less, but in all three cases there are good ion characteristics on both the ion and electron drifts sides of the probe (recall Sect. III.C. for the meaning of i-side and e-side) with no evidence for space charge effects or outgassing in the RFA cavities (the latter was a serious problem in earlier prototypes for multiple reciprocations).

In this case, the RFA is operating in classic RFA-ion mode: constant bias of V_s = -150 V on both slit plates (not shown in Fig. 8), fixed bias of around V_2 = -245 V on Grid 2 (in front of the collector - see Fig. 1) and a positive triangular, 50 Hz sweep voltage on Grid 1 from V_1 = 0 → ~220 V. At this rather low scanning frequency, the probe entrance slits move a distance of ~4.5 mm during one full voltage sweep, comparable to the 3 mm long slit which determines the minimum possible spatial resolution of the system. The collector is maintained at torus potential so that ion induced secondary electron emission is suppressed by the strong negative potential on Grid 2, though any secondaries induced via ion impact on Grid 2 will clearly be accelerated to the collector. Figure 9 illustrates two individual RFA characteristics, one each from the ion and electron sides of the probe, extracted at t = 16.56 s - the deepest point of insertion during the first reciprocation. Also included are the exponential fits performed according to Eqn. (2), demonstrating clearly that the spread of parallel ion velocities may indeed be reasonably well described by a Maxwellian distribution with characteristic temperature T_i.

Note that because the probe electronics are referenced to torus potential and not the local floating potential at the slit plate, the constant shift in the distribution, denoted V_{shift} in Fig. 9, cannot be directly related to the energy gain of ions falling through the slit plate sheath potential. To do this requires subtraction of the local floating potential, V_f, which is not measured in this case. In fact, because the saturated ion flux at the plate remains constant for all $V_s \leq V_f$, the RFA can also be run in ion mode with floating slits (at the price of allowing more primary electrons into the RFA cavity), so that V_f can be measured instantaneously and appropriately substracted from the measured V_{shift} to obtain the voltage drop across the slit. Unfortunately, it is clear in this case that the slit current is no longer measured.

The slit currents in Fig. 8 clearly show a large asymmetry from i-side to e-side (note that I_p and B_φ in Fig. 8 are in the clockwise (negative) direction, so that the i-side slit connects to field lines spiralling up from the outer divertor target) and this is naturally reflected in the collector

current ratio. In addition, the slit current envelope is reasonably symmetric about the position of minimum insertion with no strong current excursions (indicative of unipolar arcing) and demonstrating the lack of any slit plate overheating.

Such strong asymmetries are commonly observed in JET for normal (ie negative) toroidal magnetic field direction[12], and are a consequence of strong parallel field flows in the SOL, in this case in the direction from outer to inner divertor. The measurement of these flows is generally performed in JET by specific, more simple probe heads equipped with cylindrical Langmuir probe tips (which may also be used for the study of fluctuations in particle fluxes and electric fields[23] in the edge). Such measurements can sometimes be compromised by uncertainties in the collection areas of the tips and here the RFA offers the dual advantage of presenting both a well defined, rectangular surface area (24 mm^2) in the form of the exposed aperture plate and collecting a larger current.

The application of negative slit bias in RFA-ion mode (to help reject primary electrons) and the bi-directional nature of the device naturally provides a measurement of the ion saturation flux required for estimation of the flow speed past the probe. Such speeds are conventionally expressed as fractions of the ion sound speed to give a flow Mach No., M, so that $M = v_i/c_s$ with v_i the ion fluid flow velocity. There has long been considerable debate[24] about the precise relationship between the flow and the ratio of ion particle fluxes to either side of so-called "Mach probes", but the expression most often used at JET[12] is a fit to the fluid model of Hutchinson[25] giving a logarithmic function of the form:

$$M = 0.4 \ln\left(\frac{j_{sat}^{u}}{j_{sat}^{d}}\right) \qquad (4)$$

where j_{sat} is the probe ion saturation current density and the superscripts u, d denote "upstream" and "downstream" with respect to the flow which is defined as positive if it is directed towards the probe. In the case of Fig. 8, the i-side/e-side ratio is larger than unity and so the flow is directed towards the i-side and away from the e-side and thus from outer to inner divertor along the field lines.

Using Eq. (4). the experimentally measured Mach No. has been computed for the first reciprocation in Fig. 8 and is included in Fig. 10 along with the slit currents, the fitted ion temperatures and the total probe transmission factors. By convention, the data are now plotted

as a function of the distance from the position of the last closed magnetic surface at the outer midplane of the magnetic equilibrium (computed from the slit centre position). This flux mapping compresses distance by about a factor of 2 as a consequence of the stronger poloidal magnetic field at the midplane in comparison to the probe location. Since only a single T_i data point can be extracted per voltage ramp, the additional quantities in Fig. 10 are the result of averaging over the time interval corresponding to each ramp.

There is a clear trend for the i-side T_i to exceed that on the e-side for distances close to the nominal separatrix where the flow speed is highest, an effect which has recently been predicted theoretically[26] as a consequence of the modification of density and electric field profiles in the probe presheath region by the flow. For these relatively low density, ohmic plasma conditions, the measured T_i (which may be taken as an average of the upstream and downstream values) is around twice the electron temperature measured independently by Langmuir probes installed on a second reciprocating probe drive system at the same poloidal location.

The transmission factors in Fig. 10 are computed simply as the ratio $j_{sat}A_{slit}/i_{coll}$ with A_{slit} the geometric slit area and i_{coll} the measured collector current. Following the spark-erosion and laser cutting processes described in Sect. III.B, laboratory measurements revealed that the nominal slit widths (30 μm) had not been attained and were instead very close to 40 μm. In addition, the i-side slit was slightly too short (2.49 mm cf. 3.0 mm nominal) and the slit aspect ratio (width to depth) closer to 2:1 for both slits. Using the measured areas leads to the ion transmission factors of ~0.1 → 0.2 shown in Fig. 10, though it is worth noting that the slit current actually contains a component due to particle removal at the first of the three RFA grids which is in electrical contact with the slit. Assuming perfect geometric (optical) transmission at the slit and the grids, one would expect current entering the RFA to be reduced only a factor $0.81^2 \sim 0.66$ (since the first grid transmission is already included in the slit current), clearly much higher than the observed value. It is known, however, that even a knife edge slit with low aspect ratio is not perfectly transmitting in a magnetised plasma due to the helical ion motion. Matthews[10] gives analytic expressions and numerical solutions to the transmission problem for Maxwellian ions showing that transmission factors for average ion energies at values of T_i, magnetic field and slit geometry similar to those pertinent here can be of order 0.4. As described in Sect. III.B, the grids themselves, especially those with negative bias, may present somewhat lower than ideal transmission. In fact, only a further factor of 0.3 would be required to reduce the ideal geometric slit+grid transmission to the experimentally observed values in Fig. 10.

Although the RFA does operate well under certain conditions, there are important regimes under which it does not. In particular, in tests to date it appears that the device experiences difficulties even at relatively low levels of NBI power input and at higher edge densities than for the example discharge in Fig. 8. The precise reasons for the malfunction in each case are not yet fully understood, but the behaviour with increasing plasma density under low power additional heating or in ohmic heating only discharges would appear to be most likely due to the effects of space-charge with a possible, though unlikely contribution of neutral gas accumulation in the RFA cavities.

As an illustrative example, Fig. 11, is the exact analog of Fig. 8 for a discharge identical to that of Fig. 8 in every aspect save for the increase by ~50% of the plasma electron density. As a consequence, the slit and collector currents, for the same penetration distance into the SOL have increased by more than a factor 2 on both ion and electron sides, though the asymmetry and hence the strong parallel flow is maintained. Already in the first probe movement, the i-side collector current drops to negative values near the peak of the reciprocation, with the e-side, where ion fluxes are lower, unaffected. During the second insertion 2 seconds later, when the plasma density has again increased slightly, there is a clear negative current breakdown in the device on the ion side and arcing on the i-side slit. The large currents drawn at this point are sufficient to provoke strong voltage drooping on the HV power supply providing the positive sweep to Grid 1, though the voltage on the electron repelling Grid 2 is relatively unperturbed (the grids are actually separately wired in the probe head, but are driven in parallel by the HV power supply). Note, however, that normal RFA function is recovered as the probe moves further back into the SOL.

On the third reciprocation, at the highest plasma density but with reduced excursion into the plasma, arcing has ceased on the i-side slit, but the current density is still marginally higher than for the first probe movement and the resulting perturbation at the collector, whilst less marked than for the second insertion, is still higher than for the first. On the e-side, in contrast, there is evidence at the peak of the second and third reciprocations, for a slight positive offset at the collector.

Unfortunately, measurements of the individual grid currents (which are clearly significant, at least on the swept grid) are not yet available. Nevertheless, the HV swept grid power supply has a maximum current capacity of ~ 10 mA and is limited by a 10 kΩ series resistor on the output implying that the collapse, by up to ~ 100 V evident in Fig. 11 at the highest slit currents,

must be caused by grid currents of up the maximum power supply rating. For the maximum i-side slit current densities of ~2 Acm^{-2} in Fig. 11, the geometric slit transmission would provide an ion current inside the device of ~2 mA, to which must be added the residual electron current which has not been removed by the sheath and slit voltages and which must still cross the ion retarding grid before reaching the electron repeller. Ion current entering the RFA cavity might thus qualitatively account for a part of the high grid currents that are indirectly observed through the loss of grid sweep voltage at high slit currents but probably not more than ~10%.

It is instructive to assess the impact of such high currents on axial space-charge accumulation inside the RFA. Molvik[6], has reported negative current spikes at the collector once the space-charge current limit of his RFA was exceeded. In principle, this is most likely to occur in the electron-free space between the collector and electron repeller grid when the positive space-charge of the ions develops an electric field sufficient to repel ions with given axial energy. As discussed in Sect. III.B, the problem of estimating space-charge limits is non-trivial, especially in any real device. If axial space-charge is at least mostly responsible for the catastrophic loss of ion current in the example of Fig. 11, then its effect must be large enough to reflect the highest energy ions.

Adapting the expression originally derived by Langmuir[17] (Eq. (311) on pg. 244) for D^+ ions decelerated in the space from electron repeller grid to collector, Molvik gives an expression for the critical ion current density before space-charge is likely to become important that allows for a Maxwellian ion velocity distribution[6]:

$$j_{max} \approx 3.85\times10^{-8}\frac{(V_2 + E)^{3/2}}{(z - z_m)^2}[1 + 0.0247T_i^{1/2}(V_2 + E)^{-1/2}] \qquad (5)$$

where j_{max} is in Acm^{-2}, V_2 is the potential applied to the electron repeller grid, the collector is assumed to be grounded (at zero volts) and E is the axial ion energy in eV that just overcomes the positive potential hill established by the ion space charge. The quantity $(z - z_m)$ in cm, is the distance between the grid and the point of maximum potential due to the space charge and is hard to estimate. Equally, j_{max} in Eq. (5) is a current density and so comparison with the current, which is the measured quantity, requires knowledge of the beam dimension.

In a given strong magnetic field, Brillouin flow[27] will confine a non-neutral beam up to a maximum charge density of $n_B = \varepsilon_0 B^2/m_i$ which implies, for the JET RFA, that the beam area for D^+ ions with an average parallel energy of E = 100 eV (assuming T_i ~ 50 eV (Fig. 10) and

some 50 eV energy picked up during acceleration through the sheath potential drop) will be limited to the geometrical slit area only if the beam current remains below a value $i_B = en_B A_{slit}\sqrt{2E/m_i} \sim 20$ μA (B = 2 T, slit dimension 40 μm x 3 mm). This is substantially below many of the experimentally measured currents when the device functions normally. If beam expansion up to a distance of a single ion Larmor radius ($r_L = 1.02\times10^{-4}(\sqrt{m_i T_i}/Z_i B)$, with m_i the ion mass in amu, T_i in eV) is allowed for, then for T_i = 50 eV and B = 2 T, $r_L \sim 0.5$ mm, giving an approximate beam area of 0.4x0.1 cm^2, a factor of ~ 33 higher than the geometrical area. Assuming that this Larmour radus broadened value is a more realistic estimate for the slit area, and supposing that the positive space-charge potential hill peaks just in front of the collector ($(z - z_m)$ = 2 mm), Eq. (5) can be used to compute the expected maximum tolerable current at given ion energy. Inserting the appropriate values into Eq. (5) for E = 100 eV and T_i = 50 eV yields $i_{max} \sim 250$ μA rising to ~360 μA at E = 200 eV (V_2 = 240 V). These numbers increase, of course, as the potential hill moves closer to the grid, or if the current is spread over a still wider beam area (due perhaps to the effect of radial space-charge electrical fields).

It would appear from Fig. 11 that when the i-side collector currents approach values of order 100 μA, strong perturbations tend to occur. Given the rather approximate nature of the current limits computed from Eq. (5), such values are not too distant from the estimated space-charge limits, but it is very clear that the large ion currents admitted into the device at the highest slit currents considerably exceed the estimated tolerable axial space-charge limit. It is, however, far from clear why large negative collector currents should be observed if axial ion space-charge is at the origin of this effect. One possible contribution could be the production, by the reflected ions, of secondary electrons at the electron repeller grid, but this would appear unlikely to be of sufficient magnitude to explain the high negative current. Moreover, the high implied current to the swept grid cannot be explained solely by the ion current entering the device through the slit, since, even for a 2 mA incident current, a large fraction ought to be transmitted by the high transparency grid.

Large neutral fluxes inside the RFA cavity, produced by outgassing as the probe components heat up during the reciprocation or by neutrals recycled at the probe housing and entering the cavities through the pump holes might also be invoked to explain some of these features. If the neutral density increases sufficiently, a localised plasma discharge could form in the space between the entrance slit and the ion retarding grid, at which point, normal RFA function would clearly be lost. If this does occur, however, it is hard to understand how the effect can be

apparently so sensitive to the magnitude of the slit current (or particle flux density) itself - ion collector characteristics are systematically lost or are recovered when slit currents exceed or fall below a given value. Though pump-out of the RFA cavity should be rapid (Eq. (3)), thermal inertia is too slow to react on the timescales observed - even though the slit current reduces as the probe retracts, any thermal outgassing is likely to persist on longer timescales. In addition, if large neutral fluxes were entering the deviceas a result of external recycling, they should do so with equal probability on both the electron and ion-sides. There is no evidence, however, that perturbations occur on the e-side collector current - because of the net plasma flow (see above), the e-side slit current density remains at values that would likewise leave the i-side collector current unperturbed.

In future designs, the critical tolerable current density could be increased by decreasing the collector grid separation (Eq. (5)) or providing for a lower transmission, perhaps by decreasing the slit length (with the present mono-block, knife-edge design, widths much less than 20-30 μm cannot be achieved) or adding further grids. This would of course compromise measurements at lower plasma densities where space charge is not an issue. Alternatively, adding a negative bias to the collector[6] can extend the current limit, but such tests have yet to be performed in the JET device.

In general, though necessarily limited in time resolution and still difficult to use in a number of interesting operating conditions, the RFA probe head described in this contribution has reached a level of technical performance at which it has begun to provide useful physics output and has survived several hundred insertions, often beyond the separatrix and into confined plasma, without serious damage. Its successful operation, together with some useful knowledge gained in the process of optimising the probe construction, provide encouragement and support in the deployment of yet more sophisticated analysers, in particular a Plasma Ion Mass Spectrometer (PIMS) probe head[28] currently under development at JET.

ACKNOWLEDGEMENTS

The authors would particularly like to thank both the UKAEA Culham Science Centre design drafting office for some excellent design work and the CRPP mechanical workshop staff for the high quality and precision with which they manufactured the many delicate RFA components. This work was performed under the European Fusion Development Agreement and was supported in part by the Swiss National Science Foundation, EURATOM and the UK Department of Trade and Industry.

REFERENCES

[1]G. F. Matthews, J. Phys. D: Appl. Phys. **17**, 2243 (1984)

[2]R. A. Pitts, Phys. Fluids **B3**, 2873 (1991)

[3]R. A. Pitts, Contrib. Plasma Phys. **36**, 87 (1996)

[4]G. F. Matthews, R. A. Pitts, G. M. McCracken and P. C. Stangeby, Nucl. Fusion **31**, 1495 (1991)

[5]A. S. Wan, T. F. Yang, B. Lipschultz and B. LaBombard, Rev. Sci. Instrum. **57**, 1542 (1986)

[6]A. W. Molvik, Rev. Sci. Instrum. **52**, 704 (1981)

[7]S. Stephanakis and W. H. Bennett, Rev. Sci. Instrum. **39**, 1714 (1968)

[8]R. L. Stenzel, R. Williams, R. Agüero, K. Kitazaki, A. Ling, T. McDonald and J. Spitzer, Rev. Sci. Instrum. **53**, 1027 (1982)

[9]R. A. Pitts, Phd Thesis, Univ. of London. (1991)

[10]G. F. Matthews, D. Phil Thesis, Univ. of Oxford. Dept. Engineering Science (1985)

[11]S. J. Davies, S. K. Erents, A. Loarte, H. Y. Guo, G. F. Matthews, K. McCormick and R. D. Monk, Contrib. Plasma Phys. **36**, 117 (1996)

[12]S. K. Erents, A. V. Chankin, G. F. Matthews and P. C. Stangeby, Plasma Phys. Control. Fusion **42**, 905 (2000)

[13]P. C. Stangeby, J. Phys. D: Appl. Phys. **18**, 1547 (1985)

[14]H. Y. Guo, G. F. Matthews, S. J. Davies, S. K. Erents, L. D. Horton, R. D. Monk and P. C. Stangeby, Contrib. Plasma Phys. **36**, 81 (1996)

[15]G. Duesing, H. Altmann, H. Falter, A. Goede, R. Haange, S. Hemsworth, P. Kupschus, D. Stork and E. Thompson, Fusion Technology **11**, 163 (1986)

[16]R. A. Pitts and G. F. Matthews, J. Nucl. Mater. **176&177**, 877 (1990)

[17]I. Langmuir and K. T. Compton, Rev. Mod. Phys. **3**, 231 (1931)

[18]R. Nachtrieb, B. LaBombard and E. Thomas, Rev. Sci. Instrum. **71**, 4107 (2000)

[19]J. A. Simpson, Rev. Sci. Instrum. **32**, 1283 (1961)

[20]A. S. Wan, Phd Thesis, Technical Report PFC/RR-86-13, MIT Plasma Fusion Center (1986)

[21]J. D. Hobbs and J. A. Wesson, Plasma Phys. **9**, 85 (1967)

[22]J. P. Gunn, Physics of Plasmas, **8**, 1040 (2001)

[23]C. Hidalgo, B. Gonçalves, M.A. Pedrosa, C. Silva, R. Balbín, M. Hron, A. Loarte, S. K. Erents, G.F. Matthews and R. A. Pitts, J. Nucl. Mater. **313&316**, 863 (2003)

[24]G. F. Matthews, Plasma Phys. Control. Fusion **36**, 1595 (1994)

[25]I. H. Hutchinson, Phys. Fluids **B3**, 847 (1991)

[26]F. Valsaque, G. Manfredi, J. P. Gunn and E. Gauthier, Physics of Plasmas **9**, 1806 (2002)

[27]L. Brillouin, Phys. Rev. **67**, 260 (1945)

[28]G. F. Matthews. W. Schustereder, N. Cant, S. K. Erents, J. Vince, A. Qayyum, C. Mair, P. Scheier, T. D. Märk, International Journal of Mass Spectrometry **223-224**, 45 (2003)

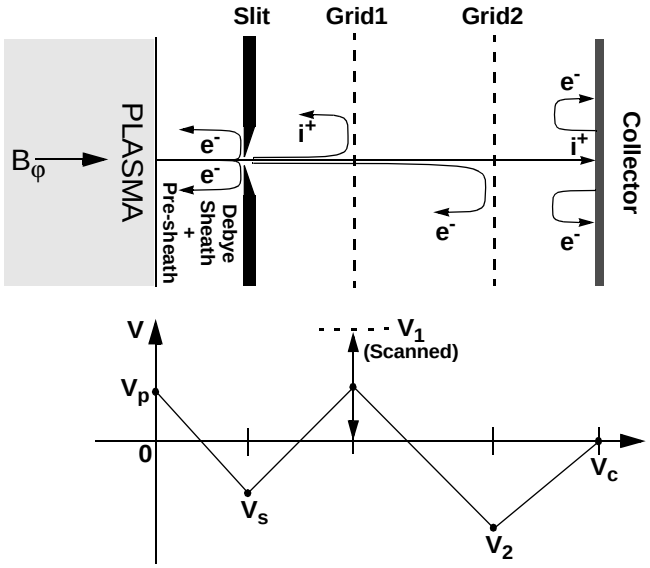

FIG. 1. Principle and bias potential arrangements for an RFA operating in ion analysis mode. The plasma is asumed to adopt some arbitrary potential, V_p, with respect to the torus ground at V = 0. The sheath and presheath potentials together place the entrance slit some $3T_e$ below V_p. Additional negative bias is applied to the slit (with respect to torus earth) to repel all but the highest energy primary electrons.

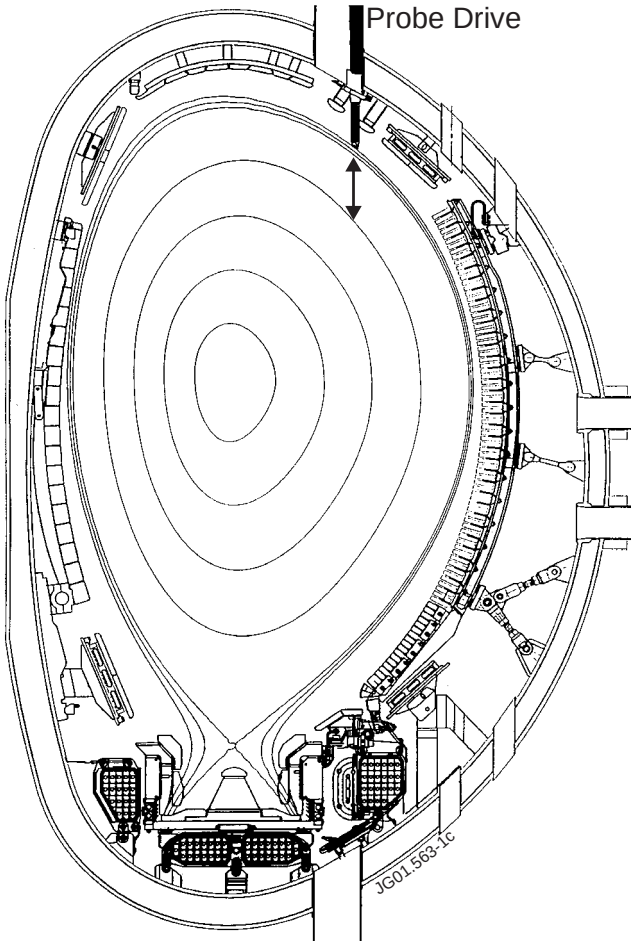

FIG. 2. Cross-section of the JET torus with representative poloidal magnetic flux surfaces for a single-null lower diverted equilibrium similar to that in which the RFA has been used. The reciprocating drive deploys the probe head from an upper, low-field-side location at a major radius of R = 3.25 m.

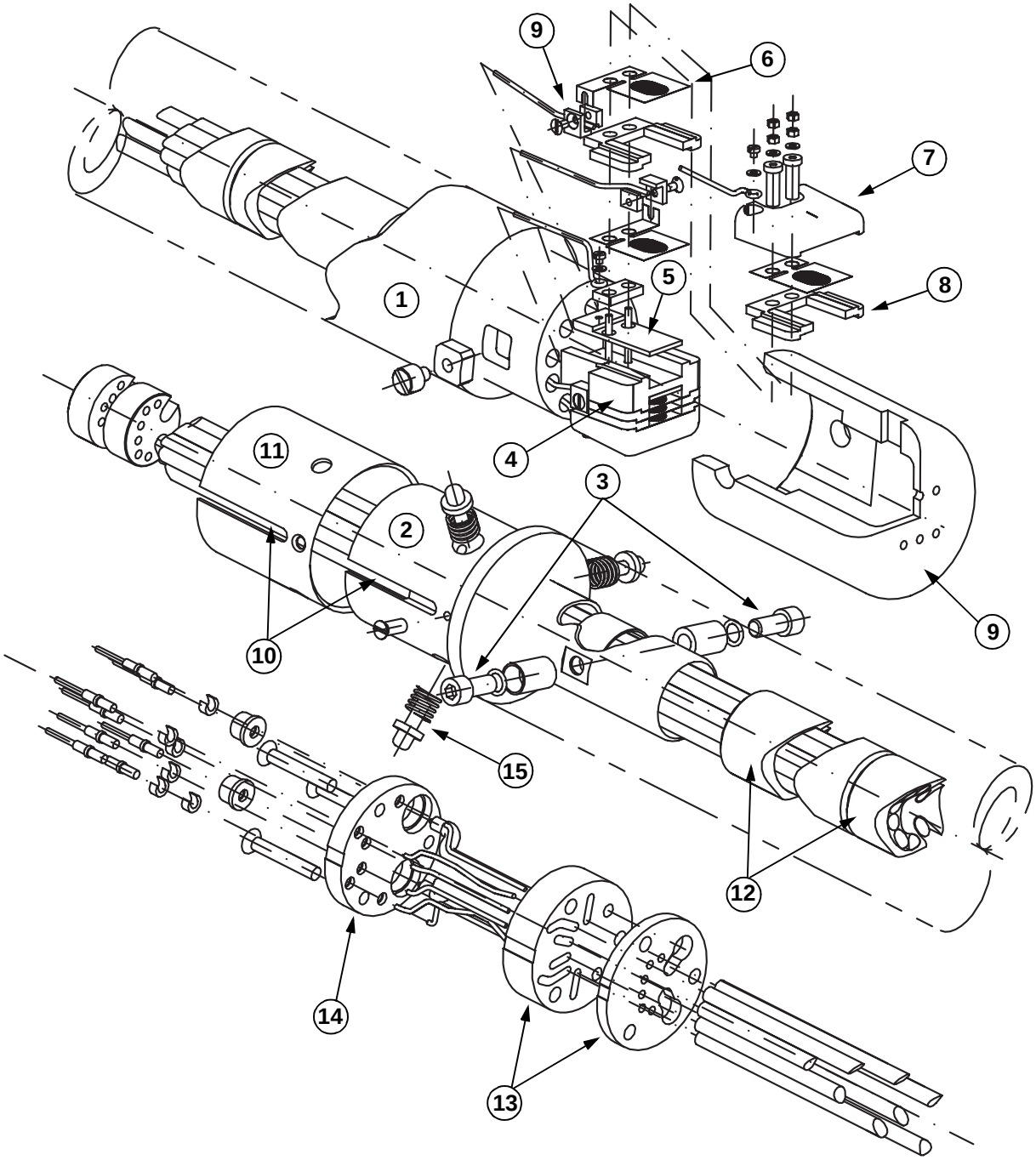

FIG. 3. Exploded, isometric decomposition of the JET RFA probe head, including details of the RFA cavities, protective housing, probe body, cable pathways and interface to the reciprocating probe drive. The numbers identify important components of the design that are described in detail throughout Sect. III.

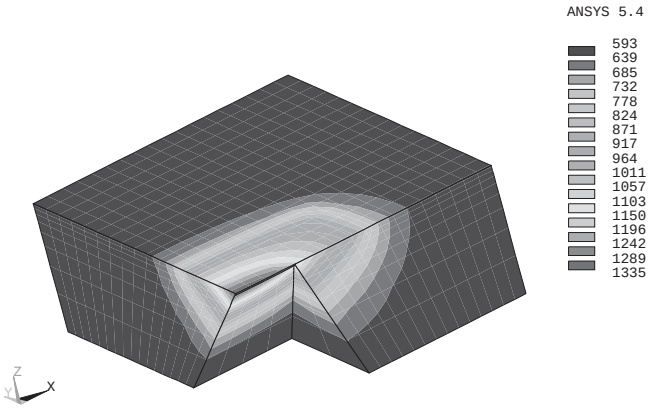

FIG. 4. Finite element simulations (ANSYS Inc., Canonsburg, USA) of a symmetric half-section of an Inconel 600 RFA slit plate treated as thermally isolated and including non-linear thermal properties. The simulation imposes a time varying plasma heat flux on an area of dimension 4x6 mm computed using real measurements from JET. The heat pulse is an approximately triangular, symmetric waveform rising from zero to a peak heat flux density of 10 MWm^{-2} in 200 ms. Starting temperature is 200°C, one of the standard JET vacuum vessel operating temperatures.

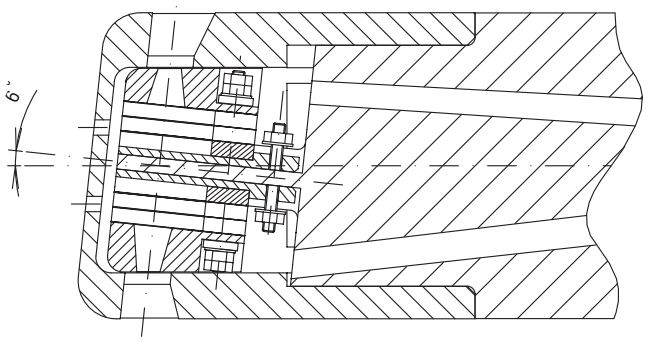

FIG. 5. Cross-section of the RFA cavity assembly illustrating the offset angle of 6° in the (φ,z) plane to account for the field line attack angle in this plane for typical discharge conditions in which the device is used.

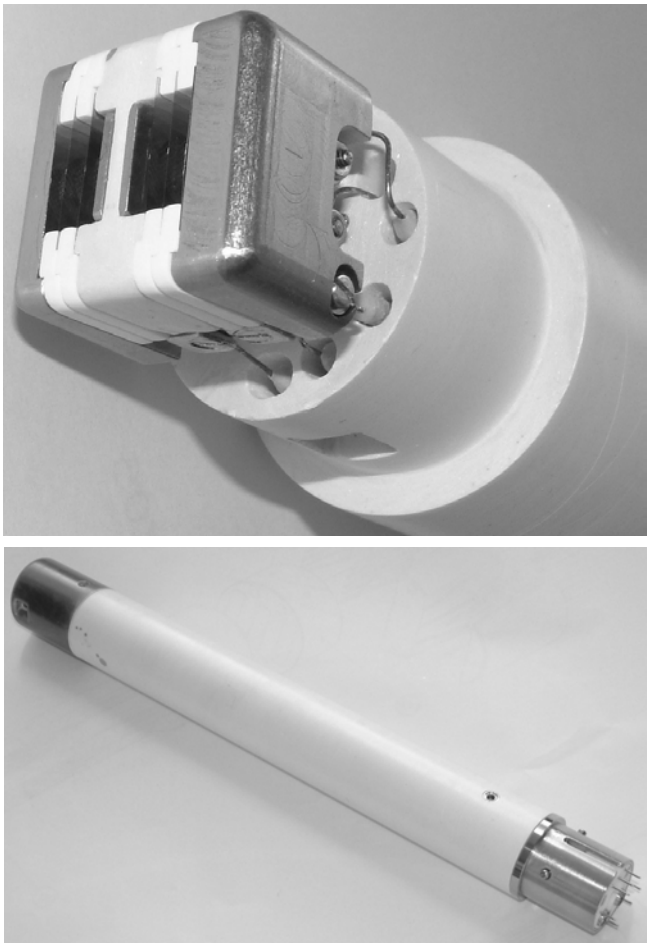

FIG. 6. Photographs of the final RFA assembly just before installation for the first experiments on JET. The tiny RFA entrance slit can just be discerned in the TZM aperture plate in the top image. From end to end, the full probe head measures 35.8 cm and has diameter 4 cm. Note, in the lower picture, the keyway in the probe drive interface for alignment in the (R,φ) plane and one of the chamfered probe housing entrance apertures just visible at top left.

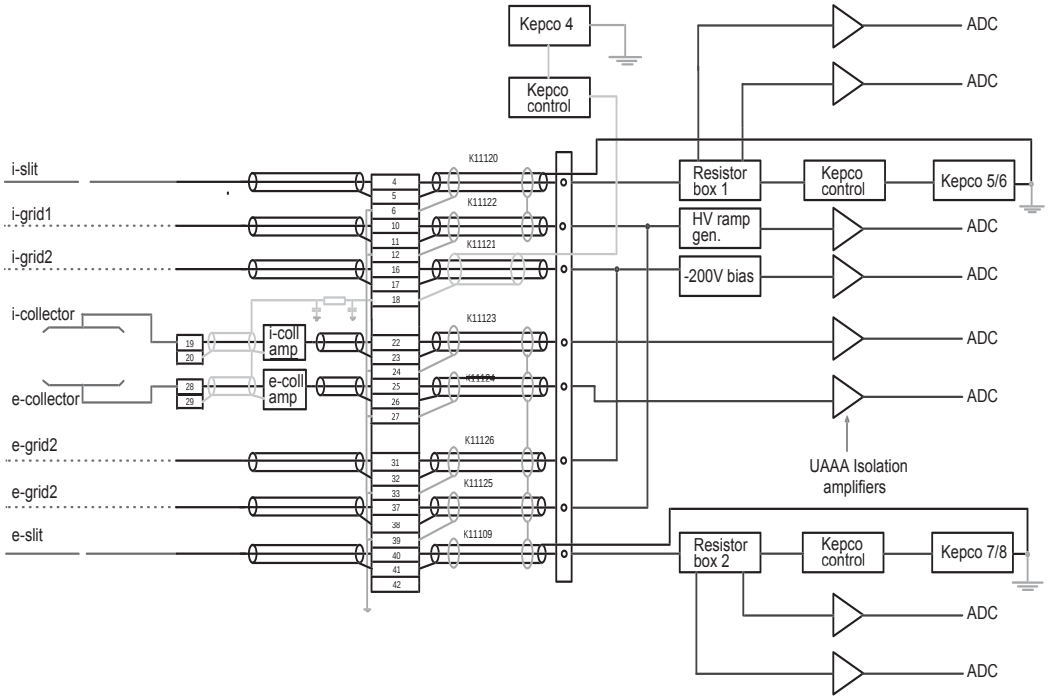

FIG. 7. Highly schematic description of RFA electronics and wiring. Note that the distance between the probe head amplifier and signal conditioning electronics/power supplies exceeds 100 m. All electronics are referenced to torus potential.

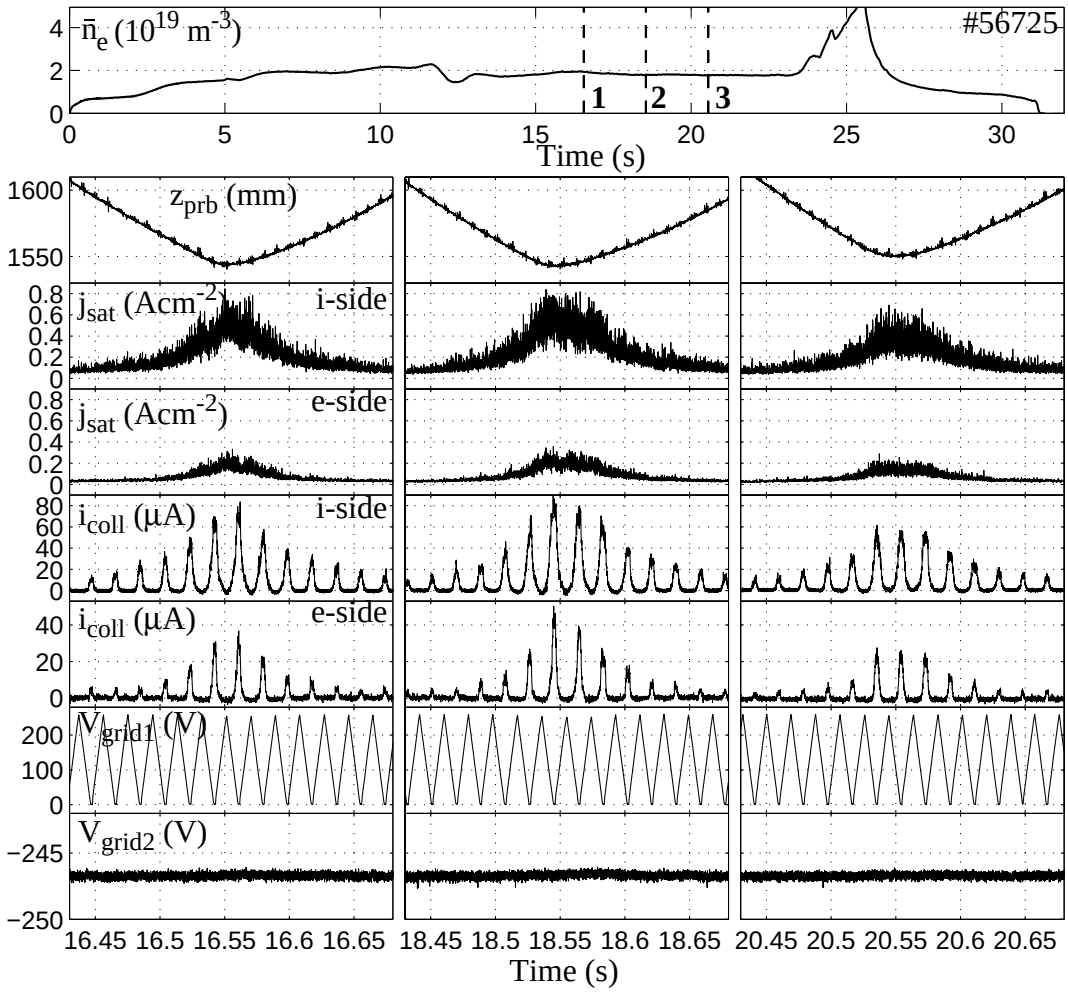

FIG. 8. Compilation of signals from the JET RFA obtained in discharge #56725, I_p = 2.0 MA, B_φ ramped in the range 2.0 → 1.5 T in the time interval 56 - 64 s. The RFA made 3 reciprocations at the times indicated by the vertical dashed lines in the top time trace, which is the plasma density averaged along a vertical chord passing through the plasma centre. Signals from each movement are plotted in the 3 columns below. The denotation i-side and e-side refers to the ion and electron drift sides of the bi-directional RFA (see text). Grids 1 and 2 have the orientation given in Fig. 1. The parameter z_{prb} is the probe height (in mm) above the vacuum vessel midplane and j_{sat} is the ion saturation current density to the entrance slit plates (held at -150 V).

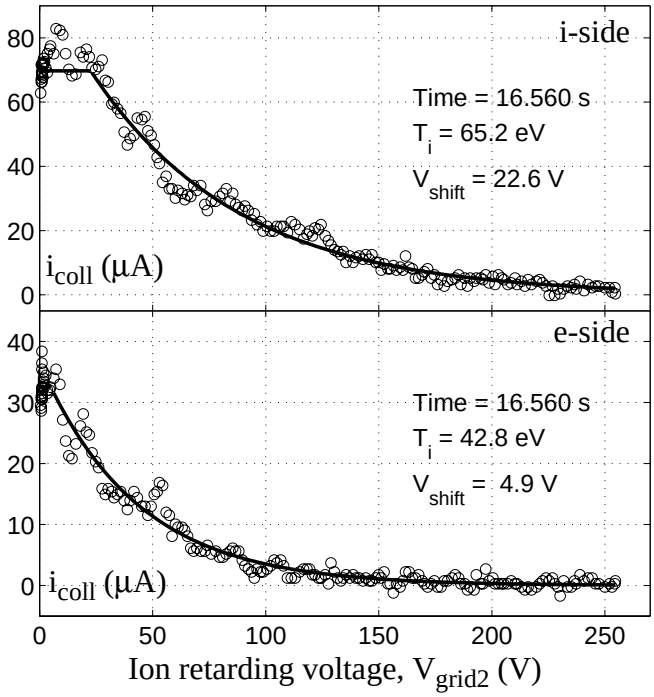

FIG. 9. Example RFA characteristics at t = 16.56 s - near the peak of the first probe reciprocation in Fig. 8. The fitted curves are obtained through an iterative procedure using Eq. (2).

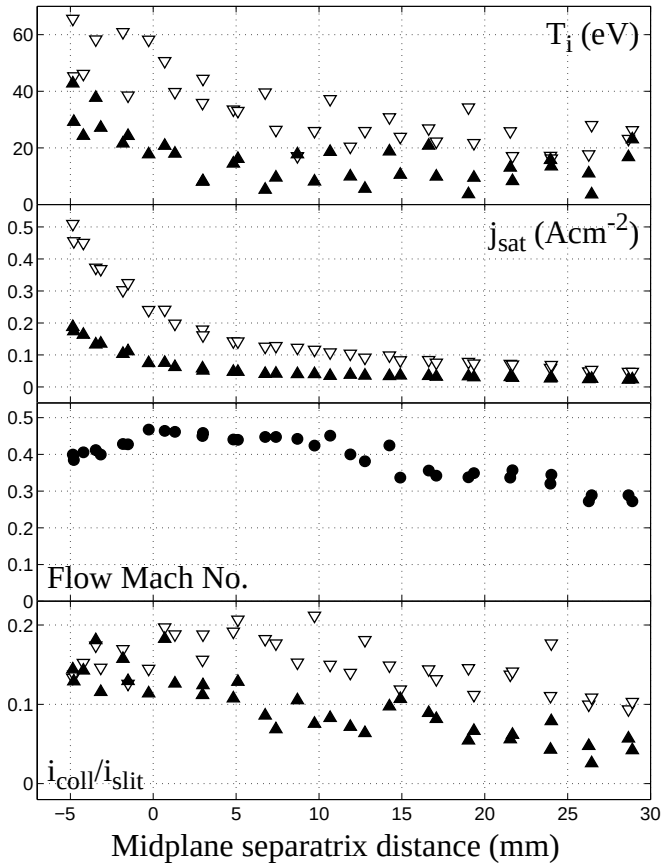

FIG. 10. Analysed data from both sides of the RFA for the first probe reciprocation in Fig. 8. Open triangles, i-side, closed triangles, e-side. The current ratio in the lower panel gives the experimentally observed total transmission. The parallel flow Mach No. is computed using Eq. (4).

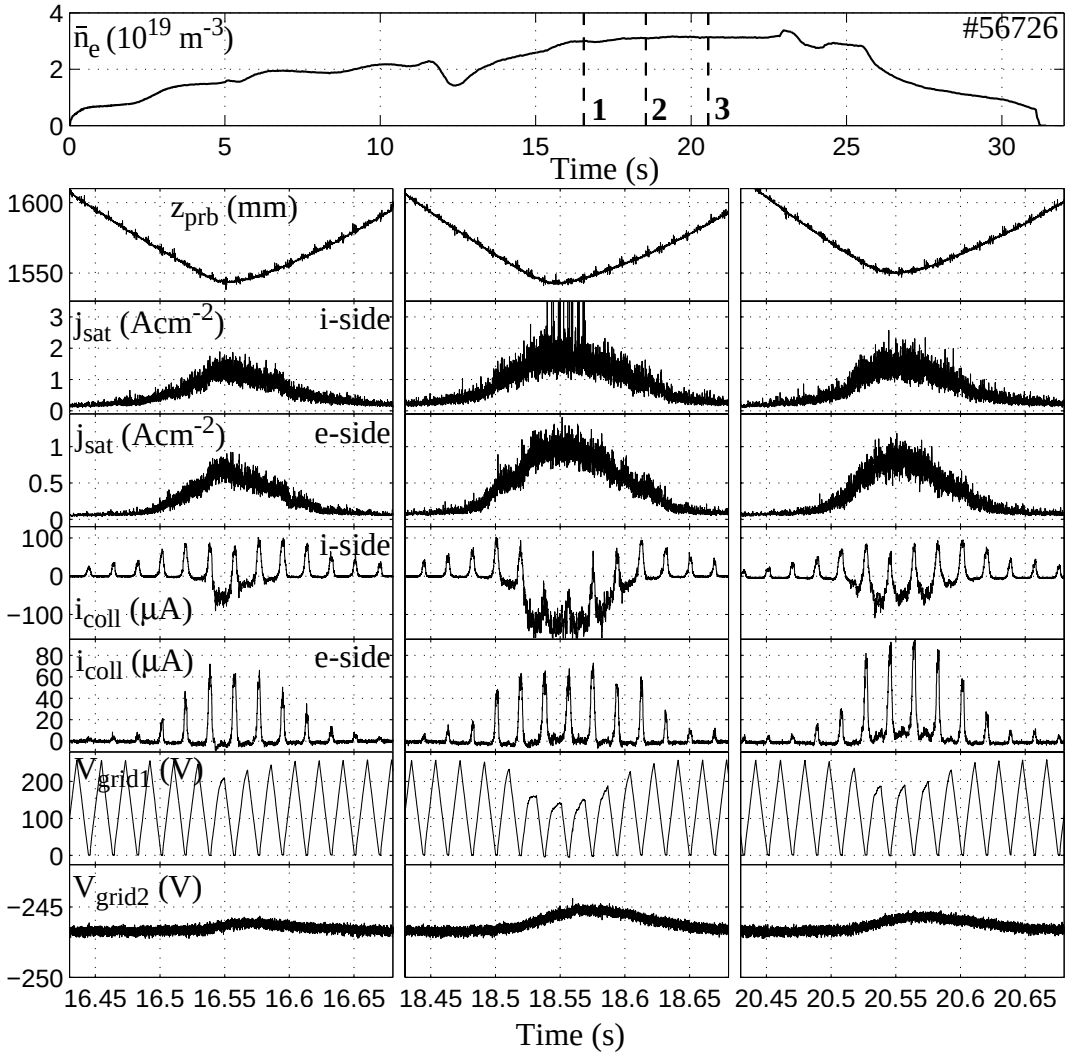

FIG. 11. RFA signals from a discharge (#56726) identical in every way to that of Fig. 8 except for the increased density waveform, which leads to apparent breakdown in the RFA i-side cavity, almost certainly due to exceeding space-charge limits. Note the strong perturbation to the ion repeller voltage, implying large (unmeasured) currents to Grid 1.